Quantum noise in optical fibers. I. Stochastic equations

P. D. Drummond

Department of Physics, The University of Queensland, St. Lucia, QLD 4072, Australia

J. F. Corney

Department of Physics, The University of Queensland, St. Lucia, QLD 4072, Australia and Department of Mathematical Modelling, Technical University of Denmark, DK-2800 Lyngby, Denmark

Received November 30, 1999; revised manuscript received May 31, 2000

We analyze the quantum dynamics of radiation propagating in a single-mode optical fiber with dispersion, nonlinearity, and Raman coupling to thermal phonons. We start from a fundamental Hamiltonian that includes the principal known nonlinear effects and quantum-noise sources, including linear gain and loss. Both Markovian and frequency-dependent, non-Markovian reservoirs are treated. This treatment allows quantum Langevin equations, which have a classical form except for additional quantum-noise terms, to be calculated. In practical calculations, it is more useful to transform to Wigner or $+P$ quasi-probability operator representations. These transformations result in stochastic equations that can be analyzed by use of perturbation theory or exact numerical techniques. The results have applications to fiber-optics communications, networking, and sensor technology. © 2001 Optical Society of America

OCIS codes: 060.4510, 270.5530, 270.3430, 190.4370, 190.5650, 060.2400.

1. INTRODUCTION

The propagation of electromagnetic radiation through optical fibers is the central paradigm of optical communications and sensor technology. It is also a novel physical system because of the material processing of fused silica, which leads to single-mode behavior with extremely low losses. Over short distances (depending on the pulse intensity) the well-known nonlinear Schrödinger (NLS) equation can describe most optical fibers with great accuracy and lead to soliton behavior as well as to many other effects. Over longer distances, a number of reservoir effects, including attenuation, Raman scattering, and the use of amplifiers and filters to compensate for losses, intervene. At the quantum level, both the original nonlinearity and the additional couplings to reservoirs can lead to quantum noise, which modifies the predictions of the classical NLS equation.

In this paper we analyze the effects of quantum noise in fiber optics. We extend and explain in more detail earlier theoretical studies in this area, which led to the prediction[1,2] and measurement[3] of intrinsic quantum-noise effects in optical solitons. The theory given here includes a detailed derivation of the relevant quantum Hamiltonian. We include quantum-noise effects that are due to nonlinearities, Raman reservoirs, and Brillouin scattering. We model the Raman–Brillouin noise by using a multiple-Lorentzian fit to measured fluorescence data, to estimate the Raman gain coefficients. Both gain and loss effects are included. This treatment is unified with the theory of gain–loss reservoirs, which was also predicted[4] and observed[5] to have large effects on soliton propagation. We treat all these reservoirs without using the Markovian approximation, to accurately treat the frequency-dependent reservoirs found in practical applications.

The purpose of this study is to lay the foundations for practical methods of calculating and numerically simulating quantum effects in nonlinear optical fibers. These effects are significant whenever quantum-limited behavior is important in communications, sensing, or measurement with optical fibers.

We introduce the basic quantum Hamiltonian for an optical fiber in Section 2. This gives a Heisenberg equation of motion that reduces to the NLS equation in the classical limit. The equation of motion is extended in Section 3 to include Raman and Brillouin effects, with gain and absorption processes considered in Section 4. The complete Heisenberg equation in Section 5 is the central result of this paper. Stochastic partial differential equations can be derived from the quantum equation by use of the phase-space methods outlined in Section 6. Applications of these methods to practical examples are reserved for a following paper.[6]

2. NONLINEAR SCHRÖDINGER MODEL

The interaction between photons in a fiber is mediated through the dielectric material that constitutes the fiber. The coupling to the dielectric introduces frequency-dependent and time-delayed behavior. The complete Hamiltonian and its derivation have been given in the literature[1,7–10]; we shall merely go over the salient points here. The starting point is a Lagrangian that generates the classical Maxwell equations for a one-dimensional di-

electric waveguide and that gives a Hamiltonian corresponding to the dielectric energy:[7]

$$H_D = \int \mathrm{d}V\left[\frac{1}{2\mu}|\mathbf{B}|^2 + \int_{t_0}^{t}\mathbf{E}(t')\cdot\dot{\mathbf{D}}(t')\mathrm{d}t'\right], \quad (2.1)$$

where the electric field $\mathbf{E} = (\mathbf{D} - \mathbf{P})/\epsilon_0$ includes the polarization response of the dielectric to an incident electric displacement $\mathbf{D}$. The field variables are then quantized by introduction of equal-time commutators between the canonical coordinates $\mathbf{D}$ and $\mathbf{B}$. We note that, of course, it is also possible to make other choices of canonical momenta. This choice corresponds to a dipole-coupled[11] rather than to a minimal-coupled fundamental Lagrangian. Whereas different Lagrangians are canonically equivalent, the present choice, originally introduced[12] by Hillery and Mlodinow in applications to dielectric theory, has the advantage of comparative simplicity. The Lagrangian must produce both the correct energy[13] and Maxwell's equations; otherwise the conjugate momenta will contain an arbitrary scaling, leading to incorrect commutation relations.[7,12]

A. Fiber-Optic Hamiltonian

The optical fiber treated will be a single transverse mode fiber with dispersion and nonlinearity. Inasmuch as boundary effects are usually negligible in experiments, it is useful first to take the infinite volume limit, which effectively replaces a summation over wave vectors with the corresponding integral. We start with a single polarization direction (i.e., a polarization-preserving fiber). The more-general case is summarized elsewhere[14] and will be treated in detail subsequently. The basic normally ordered, nonlinear Hamiltonian for the fiber in this case is[7]

$$\hat{H}_F = \int \mathrm{d}k\hbar\omega(k)\hat{a}^\dagger(k)\hat{a}(k) - \int \mathrm{d}^3\mathbf{x}\left\{\left[\frac{\Delta\chi^{(1)}(\mathbf{x})}{2\epsilon(\omega_0)}\right]:|\hat{\mathbf{D}}|^2(\mathbf{x}): + \left[\frac{\chi^{(3)}(\mathbf{x})}{4\epsilon^3(\omega_0)}\right]:|\hat{\mathbf{D}}|^4(\mathbf{x}):\right\}. \quad (2.2)$$

Here $\omega(k)$ is the angular frequency of modes with wave vector k that describes the linear polariton excitations in the fiber, including dispersion. We assume that $\omega(k)$ describes the average linear response of the fiber, in the limit of a spatially uniform environment. If the fiber is spatially nonuniform, then it is necessary to add additional inhomogeneous terms to the Hamiltonian, of generic form $\Delta\chi^{(1)}(\mathbf{x})$. As usual, $\epsilon(\omega_0)$ is the mode-average dielectric permittivity at a carrier frequency $\omega_0 = \omega(k_0)$ and $\hat{a}(k)$ is an annihilation operator, defined such that

$$[\hat{a}(k'),\hat{a}^\dagger(k)] = \delta(k - k'). \quad (2.3)$$

The coefficient $\chi^{(3)}(\mathbf{x})$ is the nonlinear coefficient that arises when the electronic polarization field is expanded as a function of the electric displacement in the commonly used Bloembergen[13] notation (the units are SI units, following current standard usage). The coefficient may vary along the longitudinal position on the fiber if the fiber has a variable composition. In terms of modes of the waveguide, and neglecting modal dispersion, the electric displacement field operator $\hat{\mathbf{D}}(\mathbf{x})$ is

$$\hat{\mathbf{D}}(\mathbf{x}) = i\int \mathrm{d}k\left\{\frac{\hbar k\epsilon[\omega(k)]v(k)}{4\pi}\right\}^{1/2}\hat{a}(k)\mathbf{u}(\mathbf{r}) \times \exp(ikx) + \text{h.c.}, \quad (2.4)$$

where

$$\int \mathrm{d}^2\mathbf{r}|\mathbf{u}(\mathbf{r})|^2 = 1. \quad (2.5)$$

Here $v(k) = \partial\omega(k)/\partial k$ is the group velocity. The function $\mathbf{u}(\mathbf{r})$ gives the transverse mode structure. Although a general mode structure can be included, for the purposes of this paper we could equally well assume a square waveguide of area A, which gives $\mathbf{u}(\mathbf{r}) \simeq \mathbf{e}_y/\sqrt{A}$. We note here that the above mode expansion for a dispersive medium is a rather general one and has been worked out both from macroscopic quantization[7] and from a microscopic model[10] with an arbitrary number of electronic or phonon resonances.

In the infinite volume limit we define the polariton field by noting that the annihilation and creation operators can be related to a quantum field by

$$\hat{\Psi}(t,x) = \frac{1}{\sqrt{2\pi}}\int \mathrm{d}k\hat{a}(t,k)\exp[i(k - k_0)x + i\omega_0 t]. \quad (2.6)$$

This photon-density operator $\hat{\Psi}(t,x)$ is the slowly varying field annihilation operator for the linear quasi-particle excitations of the coupled electromagnetic and polarization fields traveling through the fiber.[8] The nonzero equal-time commutation relations for these Bose operators are

$$[\hat{\Psi}(t,x),\hat{\Psi}^\dagger(t,x')] = \delta(x - x'). \quad (2.7)$$

As was shown in earlier treatments,[2] the Hamiltonian [Eq. (2.2)] can now be rewritten approximately as

$$\hat{H}_F = \hbar\int \mathrm{d}x\int \mathrm{d}x'\omega(x,x')\hat{\Psi}^\dagger(t,x)\hat{\Psi}(t,x') - \frac{\hbar}{2}\int \mathrm{d}x\chi^E(x)\hat{\Psi}^{\dagger 2}(t,x)\hat{\Psi}^2(t,x). \quad (2.8)$$

Here we have introduced the kernel $\omega(x,x')$, which is the linear dielectric component of the Hamiltonian, and a nonlinear coupling term $\chi^E(x)$. This kernel is then Taylor expanded about $k = k_0$ and approximated to quadratic order in $(k - k_0)$ by

$$\begin{aligned}\omega(x,x') &= \int\frac{\mathrm{d}k}{2\pi}\omega(k)\exp[i(k - k_0)(x - x')] - \frac{1}{2}k_0 v(k_0)\int \mathrm{d}^2\mathbf{r}\Delta\chi^{(1)}(\mathbf{x})|\mathbf{u}(\mathbf{r})|^2\delta(x - x') \\ &\simeq [\omega_0 + \Delta\omega(x)]\delta(x - x') + \int\frac{\mathrm{d}k}{4\pi}[i\omega_0'(\partial_{x'} - \partial_x) + \omega_0''(\partial_x\partial_{x'}) + \ldots]\exp[ik(x - x')]. \end{aligned} \quad (2.9)$$

In writing Eq. (2.8) we have assumed that the frequency dependence in the nonlinear coupling can be neglected, which is a good approximation for relatively narrow bandwidths. The nonlinear term is often called the $\chi^{(3)}$ effect, so named because it arises from the third-order term in the expansion of the polarization field in terms of the electric field.[15] It causes an electronic contribution n_{2e} to the intensity-dependent refractive index, where $n = n_0 + In_2 = n_0 + I(n_{2e} + n_{2p})$. Thus we define χ^E, in units of meters per second, as

$$\chi^E(x) \equiv \left[\frac{3\hbar\omega_0{}^2 v(k_0)^2}{4\epsilon(\omega_0)c^2}\right]\int \mathrm{d}^2\mathbf{r}\chi^{(3)}(\mathbf{x})|\mathbf{u}(\mathbf{r})|^4 \equiv \left[\frac{\hbar n_{2e}(x)\omega_0{}^2 v^2}{Ac}\right]. \tag{2.10}$$

Here $A = [\int \mathrm{d}^2\mathbf{r}|\mathbf{u}(\mathbf{r})|^4]^{-1}$ is the effective modal cross section and n_{2e} is the refractive-index change per unit field intensity that is due to electronic transitions. It is less than the total value observed for n_2, as phonon contributions have yet to be included.

The free evolution part of the total Hamiltonian, which will be removed in subsequent calculations, just describes the carrier frequency ω_0. It is not needed in Heisenberg picture calculations for $\hat{\Psi}(t,x)$ because it is canceled by the slowly varying field definition. Next, on partial integration of the derivative terms and Fourier transforming, the resultant interaction Hamiltonian $\hat{H}_F{}'$ that describes the evolution of $\hat{\Psi}$ in the slowly varying envelope and rotating-wave approximations is

$$\hat{H}_F{}' = \hat{H}_F - \int \mathrm{d}k\hbar\omega_0\hat{a}^\dagger(k)\hat{a}(k) = \frac{\hbar}{2}\int_{-\infty}^{\infty}\mathrm{d}x\left[\Delta\omega(x)\hat{\Psi}^\dagger\hat{\Psi} + \frac{iv}{2}(\nabla\hat{\Psi}^\dagger\hat{\Psi} - \hat{\Psi}^\dagger\nabla\hat{\Psi}) + \frac{\omega''}{2}\nabla\hat{\Psi}^\dagger\nabla\hat{\Psi} - \frac{\chi^E(x)}{2}\hat{\Psi}^{\dagger 2}\hat{\Psi}^2\right]. \tag{2.11}$$

For simplicity, only quadratic dispersion is included here. However, the extension to higher-order dispersion is relatively straightforward. It can be achieved by inclusion of higher-order terms in the expansion of the dielectric kernel or else by treatment of the dispersion as part of the reservoir response function, as in what follows. The response function approach has the advantages that a completely arbitrary polarization response can be included and that transformations to a different frame of reference are simplified. If part of the dielectric response is treated with response functions, then this part of the measured refractive index must be excluded from the free Hamiltonian to avoid double counting.

B. Heisenberg Equation

From the interaction Hamiltonian [Eq. (2.11)] we find the following Heisenberg equation of motion for the field operator propagating in the $+x$ direction:

$$\left(v\frac{\partial}{\partial x} + \frac{\partial}{\partial t}\right)\hat{\Psi}(t,x) = \left[-i\Delta\omega(x) + \frac{i\omega''}{2}\frac{\partial^2}{\partial x^2} + i\chi^E(x)\hat{\Psi}^\dagger(t,x)\hat{\Psi}(t,x)\right]\hat{\Psi}(t,x). \tag{2.12}$$

This is the quantum NLS equation in the laboratory frame of reference, which is completely equivalent to the theory of a Bose gas of massive quasi-particles with an effective mass of $\hbar/\omega''$ and an average velocity of v for photons near the carrier frequency of interest. It includes the possibility that the dielectric constant (i.e., the linear response) has a spatial variation, through the term $\Delta\omega(x)$.

We note here that it is occasionally assumed that operators obey equal-space, rather than equal-time, commutation relations. This cannot be exactly true, because commutators in an interacting quantum field theory are well defined only at equal times. At different times, it is possible for a causal effect to propagate to a different spatial location, which can therefore change the unequal-time commutator. In other words, imposing free-field equal-space but unequal-time commutators is not strictly compatible with causality. The assumption of equal-space commutators may be used as an approximation under some circumstances, provided that interactions are weak. In this paper we shall use standard equal-time commutators.

3. RAMAN HAMILTONIAN

To the Hamiltonian given in Eq. (2.11) must be added couplings to linear gain, absorption, and phonon reservoirs.[16–18] The gain and absorption reservoirs are discussed at length in Section 4 below. The phonon field consists of thermal and spontaneous excitations in the displacement of atoms from their mean locations in the dielectric lattice. Although previous quantum treatments of Raman scattering have been given,[19] it is necessary to modify them somewhat in the present situation. The Raman interaction energy[16,20] of a fiber, in terms of atomic displacements from mean lattice positions, is known to have the form

$$H_R = \frac{1}{2}\sum_j \eta_j^R \vdots \mathbf{D}(\bar{\mathbf{x}}^j)\mathbf{D}(\bar{\mathbf{x}}^j)\,\delta\mathbf{x}^j + \frac{1}{2}\sum_{ij}\kappa_{ij}\vdots\delta\mathbf{x}^i\,\delta\mathbf{x}^j. \tag{3.1}$$

Here $\mathbf{D}(\bar{\mathbf{x}}^j)$ is the electric displacement at the jth mean atomic location $\bar{\mathbf{x}}^j$, $\delta\mathbf{x}^j$ is the atomic displacement operator, η_j^R is a Raman coupling tensor, and κ_{ij} represents the short-range atom–atom interactions.

To quantize this interaction with atomic positions, using our macroscopic quantization method, we must now take into account the existence of a corresponding set of phonon operators, $\hat{b}(\omega,x)$ and $\hat{b}^\dagger(\omega,x)$. These operators diagonalize the atomic displacement Hamiltonian in each fiber segment and have well-defined eigenfrequencies. There are calculations[21] of the frequency spectrum and normal modes of vibration for vitreous silica that use physical models based on the random network theory of

disordered systems. The computed vibrational frequency spectrum is remarkably similar to the observed Raman gain profile.[22] The phonon–photon coupling induces Raman transitions and scattering from acoustic waves (the Brillouin effect), resulting in extra noise sources and an additional contribution to the nonlinearity. The initial state of phonons is thermal, with $n_{\mathrm{th}}(\omega) = [\exp(\hbar\omega/kT)-1]^{-1}$.

A. Hamiltonian and Heisenberg Equations

In terms of these phonon operators, the fiber Hamiltonian in the interaction picture and within the rotating-wave approximation for a single polarization is[16] $\hat{H}' = \hat{H}_R + \hat{H}_{F'}$, where we have introduced a Raman interaction Hamiltonian:

$$\hat{H}_R = \hbar\int_{-\infty}^{\infty}\mathrm{d}x\int_0^{\infty}\mathrm{d}\omega\{\hat{\Psi}^{\dagger}(x)\hat{\Psi}(x)R(\omega,x) \times [\hat{b}(\omega,x)+\hat{b}^{\dagger}(\omega,x)] + \omega\hat{b}^{\dagger}(\omega,x)\hat{b}(\omega,x)\}. \quad (3.2)$$

Here the atomic vibrations within the silica structure of the fiber are modeled as a continuum of localized oscillators and are coupled to the radiation modes by a Raman transition with a real frequency-dependent coupling $R(\omega,x)$. This coupling could be nonuniform in space and is determined empirically through measurements of the Raman gain spectrum.[16] The atomic displacement is proportional to $\hat{b}+\hat{b}^{\dagger}$, where the phonon annihilation and creation operators, $\hat{b}$ and $\hat{b}^{\dagger}$, have the equal-time commutations relations

$$[\hat{b}(t,\omega,x),\,\hat{b}^{\dagger}(t,\omega',x')] = \delta(x-x')\delta(\omega-\omega'). \quad (3.3)$$

Thus the Raman excitations are treated as an inhomogeneously broadened continuum of modes, localized at each longitudinal location x. Guided wave acoustic Brillouin scattering[23–26] is a special case of this, in the low-frequency limit. Because neither Raman nor Brillouin excitations are completely localized, this treatment requires a frequency and wave-number cutoff such that the field operator $\hat{\Psi}$ is slowly varying on the phonon scattering distance scale. The corresponding coupled nonlinear operator equations are

$$\left(v\frac{\partial}{\partial x}+\frac{\partial}{\partial t}\right)\hat{\Psi}(t,x) = i\Bigg[-\Delta\omega(x)+\frac{\omega''}{2}\frac{\partial^2}{\partial x^2} + \chi^{E}(x)\hat{\Psi}^{\dagger}(t,x)\hat{\Psi}(t,x)\Bigg]\hat{\Psi}(t,x) - i\Bigg\{\int_0^{\infty}R(\omega,x)[\hat{b}(t,\omega,x) + \hat{b}^{\dagger}(t,\omega,x)]\mathrm{d}\omega\Bigg\}\hat{\Psi}(t,x),$$

$$\frac{\partial}{\partial t}\hat{b}(t,\omega,x) = -i\omega\hat{b}(t,\omega,x) - iR(\omega,x)\hat{\Psi}^{\dagger}(t,x)\hat{\Psi}(t,x). \quad (3.4)$$

In summary, the original theory of nonlinear quantum field propagation is now extended to include both the electronic and the Raman nonlinearities. The result is a modified Heisenberg equation with a delayed nonlinear response to the field that is due to the Raman coupling. On integrating the Raman reservoirs, one obtains

$$\left(v\frac{\partial}{\partial x}+\frac{\partial}{\partial t}\right)\hat{\Psi}(t,x) = i\Bigg[-\Delta\omega(x)+\frac{\omega''}{2}\frac{\partial^2}{\partial x^2} + \int_{0-}^{\infty}\mathrm{d}t'\chi(t',x) \times[\hat{\Psi}^{\dagger}\hat{\Psi}](t-t',x) + \hat{\Gamma}^{R}(t,x)\Bigg]\hat{\Psi}(t,x),$$

where

$$\chi(t,x) = \chi^{E}(x)\delta(t) + 2\Theta(t)\int_0^{\infty}R^2(\omega,x)\sin(\omega t)\mathrm{d}\omega,$$

$$\hat{\Gamma}^{R}(t,x) = -\int_0^{\infty}R(\omega,x)[\hat{b}(t,\omega,x)+\hat{b}^{\dagger}(t,\omega,x)]\mathrm{d}\omega, \quad (3.5)$$

in which we have defined $\Theta(t)$ as the step function.

The operators $\hat{\Gamma}^{R}$ and $\hat{\Gamma}^{R\dagger}$ are stochastic, with Fourier transforms defined by use of the normal Fourier-transform conventions for field operators:

$$\hat{\Gamma}^{R}(\omega,x) = \frac{1}{\sqrt{2\pi}}\int\mathrm{d}t\,\exp(i\omega t)\hat{\Gamma}^{R}(t,x), \quad (3.6)$$

$$\hat{\Gamma}^{R\dagger}(\omega,x) = \frac{1}{\sqrt{2\pi}}\int\mathrm{d}t\,\exp(-i\omega t)\hat{\Gamma}^{R}(t,x). \quad (3.7)$$

The frequency–space correlations are given by

$$\langle\hat{\Gamma}^{R\dagger}(\omega',x')\hat{\Gamma}^{R}(\omega,x)\rangle = 2\chi''(x,|\omega|) \times[n_{\mathrm{th}}(|\omega|)+\Theta(-\omega)] \times\delta(x-x')\delta(\omega-\omega'). \quad (3.8)$$

In Eq. (3.8) we introduce a Raman amplitude gain of χ'' per unit photon flux, equal to the imaginary part of the Fourier transform of $\chi(t,x)$, such that $\chi''(x,|\omega|) = \pi R^2(x,|\omega|)$. Here we use the Bloembergen normalization for response function Fourier transforms:

$$\tilde{\chi}(\omega,x) = \int\mathrm{d}t\,\exp(i\omega t)\chi(t,x), \quad (3.9)$$

which does not include the $\sqrt{2\pi}$ factor.

Of some significance is the physical interpretation of the correlation functions, which can be regarded as contributing directly to the normally ordered spectrum of the transmitted field. Given a cw carrier, the correlations when ω is positive correspond to an anti-Stokes (blue-shifted) spectral term, which is clearly zero unless the thermal phonon population is appreciable. However, when ω is negative, the theta function term indicates that the Stokes (redshifted) spectral term is nonzero, owing to spontaneous Stokes photons emitted even at zero temperature.

B. Raman Gain Measurements

The measured intensity gain that is due to Raman effects at a given relative frequency ω per unit length, per unit carrier photon flux $I_0 = v\langle\hat{\Psi}^\dagger\hat{\Psi}\rangle$, is

$$\frac{1}{I_0}\frac{\partial \ln I}{\partial x} = -2\chi''(\omega, x)/v^2. \tag{3.10}$$

Here the gain is positive for Stokes-shifted frequencies ($\omega < 0$) and negative for anti-Stokes ($\omega > 0$), as one would expect. This relationship allows the coupling to be estimated from measured Raman gain and fluorescence properties. The simplest way to achieve this goal is to expand the Raman response function in terms of a multiple-Lorentzian model, which can then be fitted to observed Raman fluorescence data by a nonlinear least-squares fit. We therefore expand

$$\chi(t, x) = \chi^E(x)\delta(t) + \chi(x)\Theta(t)\sum_{j=0}^{n} F_j\delta_j \exp(-\delta_j t)\sin(\omega_j t). \tag{3.11}$$

For normalization purposes, we have introduced $\chi(x)$, which is defined as the total effective nonlinear phase-shift coefficient per unit time and photon density, in units of radius times meters per second, obtained from the low-frequency nonlinear refractive index. The coefficient is given in terms of the electronic or fast-responding nonlinear coefficient $\chi^E(x)$, together with the Raman contribution, by integration over time:

$$\chi(x) = \chi^E(x) + 2\int_0^\infty\int_0^\infty R^2(\omega, x)\sin(\omega t)\mathrm{d}\omega\mathrm{d}t. \tag{3.12}$$

In the above expansion, F_j are a set of dimensionless Lorentzian strengths and ω_j and δ_j are the resonant frequencies and widths, respectively, of the effective Raman resonances at each frequency. To improve convergence, we do not constrain the Lorentzian strength parameters to be positive. The $j = 0$ Lorentzian models the Brillouin contribution to the response function. In general, all these parameters could be x dependent, but for notational simplicity we often assume that they are constant in space. The values for an $n = 10$ fit in the case of a typical fused-silica fiber are given in Table 1, including an estimate of the effective Brillouin contribution averaged over the individual Brillouin scattering peaks. The coefficient of the electronic nonlinearity is now obtained explicitly in terms of the total nonlinear refractive index:

$$\chi^E(x) = \frac{\hbar(1-f)n_2{\omega_0}^2v^2}{Ac}, \tag{3.13}$$

where ω_0 is the carrier frequency, A is the effective cross-sectional area of the traveling mode, and f is the fraction of the nonlinearity that is due to the Raman gain, which has been estimated from the procedure outlined above:

$$f = \frac{\chi^R}{\chi} = \frac{2}{\chi}\int_0^\infty \mathrm{d}t\int_0^\infty \mathrm{d}\omega R^2(\omega, x)\sin(\omega t) \simeq 0.2. \tag{3.14}$$

A result of this model is that the phonon operators do not have white-noise behavior. In fact, this colored noise property is significant enough to invalidate the usual Markovian and rotating-wave approximations, which are therefore not used in the phonon equations. Of course, the photon modes may also be in a thermal state of some type. However, thermal effects are typically much more important at the low frequencies that characterize Raman and Brillouin scattering than they are at optical frequencies. In addition, if the input is a photon field generated by a laser, any departures from coherent statistics will be rather specific to the laser type, rather than having the generic properties of thermal fields.

Finally, there is another effect that has so far been neglected. This is the ultralow-frequency tunneling that is due to lattice defects.[27] As this effect is not strictly linear, it cannot be included accurately in our macroscopic Hamiltonian. Despite this, the effects of this $1/f$ type of noise may be included approximately for any predetermined temperature. One can achieve this inclusion by simply modifying the refractive-index perturbation term such that it becomes $\Delta\omega(t, x)$ and generates the known low-frequency refractive-index fluctuations.

4. GAIN AND ABSORPTION

In silica optical fibers there is a relatively flat absorption profile, with a minimum absorption coefficient of approximately 0.2 dB/km in the vicinity of the commonly used communications wavelengths of $\sim\lambda = 1.5\,\mu$m. This effect can be compensated for by the use of fiber laser amplifiers, resulting in nearly zero net absorption over a total link that includes both normal and amplified fiber segments. In practical terms, this situation leads to an approximately uniform fiber environment, provided that the net gain and loss are spatially modulated more rapidly than is the pulse dispersion length. These additional effects need to be included within the present Hamiltonian model for a fully consistent quantum theory. For wideband communications systems with either time-domain multiplexing or frequency-domain multiplexing, it can become necessary to include the frequency dependence and spatial variation of the gain and loss terms. This is especially true if spectral filters are included in the fiber.

Table 1. Fitting Parameters for the 11-Lorentzian Model of the Raman Gain Function $h^R(t/t_0)$[a]

j	F_j	ω_j	δ_j
0	0.16	0.005	0.005
1	−0.3545	0.3341	8.0078
2	1.2874	26.1129	46.6540
3	−1.4763	32.7138	33.0592
4	1.0422	40.4917	30.2293
5	−0.4520	45.4704	23.6997
6	0.1623	93.0111	2.1382
7	1.3446	99.1746	26.7883
8	−0.8401	100.274	13.8984
9	−0.5613	114.6250	33.9373
10	0.0906	151.4672	8.3649

[a] All frequencies are in Terarad/s.

A. Absorbing Reservoirs

The absorption reservoir is modeled most simply by a coupling to a continuum of harmonic oscillators at resonant frequency ω. In the interaction picture used here, the Hamiltonian term that causes rapidly varying operator evolution of the reservoir at carrier frequency ω_0 is subtracted, leaving

$$\hat{H}_A{}' = \hbar \int_{-\infty}^{\infty} \mathrm{d}x \int_0^{\infty} \mathrm{d}\omega \{[\hat{\Psi}(x)\hat{a}^{\dagger}(\omega, x)A(\omega, x) + \mathrm{h.c.}] + (\omega - \omega_0)\hat{a}^{\dagger}\hat{a}(\omega, x)\}, \tag{4.1}$$

where $A(\omega, x)$ provides the frequency-dependent coupling between the radiation modes and the absorption reservoirs. The reservoir annihilation and creation operators, $\hat{a}$ and $\hat{a}^{\dagger}$, have the commutation relations

$$[\hat{a}(\omega, x), \hat{a}^{\dagger}(\omega', x')] = \delta(x - x')\delta(\omega - \omega'). \tag{4.2}$$

The equations for the absorbing photon reservoirs can be integrated immediately. The photon reservoir variable, for instance, obeys

$$\frac{\partial}{\partial t}\hat{a}(t, \omega, x) = -i(\omega - \omega_0)\hat{a}(t, \omega, x) - iA(\omega, x)\hat{\Psi}(t, x). \tag{4.3}$$

Hence the solutions are

$$\hat{a}(t, \omega, x) = \hat{a}(t_0, \omega, x)\exp[-i(\omega - \omega_0)(t - t_0)] - iA(\omega, x)\int_{t_0}^{t} \exp[-i(\omega - \omega_0) \times (t - t')]\hat{\Psi}(t', x)\mathrm{d}t', \tag{4.4}$$

with initial correlations for the reservoir variables in the far past ($t_0 \to -\infty$) given by

$$\langle \hat{a}^{\dagger}(t_0, \omega, x)\hat{a}(t_0, \omega', x')\rangle = n_{\mathrm{th}}(\omega)\delta(x - x')\delta(\omega - \omega'),$$
$$\langle \hat{a}(t_0, \omega, x)\hat{a}^{\dagger}(t_0, \omega', x')\rangle = [n_{\mathrm{th}}(\omega) + 1] \times \delta(x - x')\delta(\omega - \omega'). \tag{4.5}$$

The solution for $\hat{a}(t, \omega, x)$ is substituted into the Heisenberg equation for the field evolution, giving rise to an extra time-dependent term of the form

$$\begin{aligned} -i\int_0^{\infty} A^*(\omega, x)\hat{a}(t, \omega, x)\mathrm{d}\omega &= -\int_0^{\infty} \mathrm{d}\omega |A(\omega, x)|^2 \int_{t_0}^{t} \mathrm{d}t' \exp[-i(\omega - \omega_0)(t - t')] \times \hat{\Psi}(t', \omega) - i\int_0^{\infty} \mathrm{d}\omega A^*(\omega, x)\exp[-i(\omega - \omega_0) \times (t - t_0)]\hat{a}(t_0, \omega, x) \\ &= -\int_0^{\infty} \mathrm{d}t'' \gamma^A(t'', x)\hat{\Psi}(t - t'', x) + \hat{\Gamma}^A(t, x), \end{aligned} \tag{4.6}$$

where $t'' = t - t'$ and we obtain the response function and reservoir terms most simply by extending the lower limit on the frequency integral to $-\infty$, introducing only an infinitesimal error in the process, such that

$$\gamma^A(t, x) \approx \Theta(t)\int_{-\infty}^{+\infty} \mathrm{d}\omega |A(\omega, x)|^2 \exp[-i(\omega - \omega_0)t],$$

$$\hat{\Gamma}^A(t, x) = -i\int_0^{\infty} \mathrm{d}\omega A^*(\omega, x)\exp[-i(\omega - \omega_0)(t - t_0)] \times \hat{a}(t_0, \omega, x). \tag{4.7}$$

The response function integral represents a deterministic, or drift, term to the motion, with a Fourier transform of

$$\tilde{\gamma}^A(\omega, x) = \int \gamma^A(t, x)\exp(i\omega t)\mathrm{d}t = \gamma^A(\omega, x) + i\gamma^{A\prime\prime}(\omega, x), \tag{4.8}$$

so the amplitude loss rate is

$$\gamma^A(\omega, x) = \pi |A(\omega_0 + \omega, x)|^2. \tag{4.9}$$

In the case of a spatially uniform reservoir with a flat spectral density, the Wigner–Weiskopff approximation (neglecting frequency shifts) gives a uniform Markovian loss term with

$$\gamma^A(t) \approx \tilde{\gamma}^A\delta(t), \tag{4.10}$$

where the average amplitude loss coefficient is

$$\tilde{\gamma}^A = \tilde{\gamma}^A(0) = \int_0^{\infty}\int_{-\infty}^{+\infty} \mathrm{d}t\mathrm{d}\omega |A(\omega)|^2 \exp[-i(\omega - \omega_0)t] = \gamma^A + i\gamma^{A\prime\prime}. \tag{4.11}$$

This approximation, known as the Markov approximation, is generally rather accurate for the absorbing reservoirs, whose response does not typically vary fast with frequency. Exceptions to this rule would be any case involving resonant impurities in the fiber or very short pulses whose bandwidths are comparable with the frequency scale of absorption changes.

The second quantity in expressions (4.7), $\hat{\Gamma}^A(t, x)$, behaves as a stochastic term owing to the random initial conditions. Neglecting the frequency dependence of the thermal photon number yields the corresponding correlation functions

$$\begin{aligned} \langle \hat{\Gamma}^A(t, x)\hat{\Gamma}^{A\dagger}(t', x')\rangle &= \int_0^{\infty} \mathrm{d}\omega |A(\omega, x)|^2 \exp[-i(\omega - \omega_0)(t - t')] \times [n_{\mathrm{th}}(\omega) + 1]\delta(x - x') \\ &\approx [\gamma^A(t - t', x) + \gamma^{A*}(t' - t, x)] \times [n_{\mathrm{th}}(\omega_0) + 1]\delta(x - x'), \end{aligned} \tag{4.12}$$

$$\langle \hat{\Gamma}^{A\dagger}(t',x')\hat{\Gamma}^{A}(t,x)\rangle = \int_0^\infty \mathrm{d}\omega |A(\omega,x)|^2 \exp[-i(\omega-\omega_0) \times (t-t')] n_{\mathrm{th}}(\omega)\delta(x-x') \approx [\gamma^A(t-t',x) + \gamma^{A*}(t'-t,x)] \times n_{\mathrm{th}}(\omega_0)\delta(x-x'). \quad (4.13)$$

At optical or infrared frequencies it is a good approximation to set $n_{\mathrm{th}}(\omega_0)=0$. On Fourier transforming the noise sources, one obtains

$$\langle \hat{\Gamma}^{A}(\omega,x)\hat{\Gamma}^{A\dagger}(\omega',x')\rangle = 2\gamma^A(\omega,x)\delta(x-x')\delta(\omega-\omega'). \quad (4.14)$$

Again taking the simplifying case of a spatially uniform reservoir in the Wigner–Weiskopff limit reduces Eq. (4.14) to

$$\langle \hat{\Gamma}^{A}(t,x)\hat{\Gamma}^{A\dagger}(t',x')\rangle = 2\gamma^A\delta(t-t')\delta(x-x'), \quad \langle \hat{\Gamma}^{A\dagger}(t,x)\hat{\Gamma}^{A}(t',x)\rangle = 0. \quad (4.15)$$

Note that the dimensions for the amplitude relaxation rates γ^A are inverse tune. It is easy to show that $2\gamma^A/v$ corresponds to the usual linear absorption coefficient for fibers during propagation. A typical measured absorption figure in current fused-silica communications fibers is 0.2 dB/km in the minimum region of absorption (near $\lambda = 1.5\,\mu$m). The corresponding absorption coefficient is $2\gamma^A/v \simeq 2.3\times 10^{-5}\,\mathrm{m}^{-1}$. To the extent that this effect is wavelength (and hence frequency) dependent, the resultant dispersion can be included as well, giving rise to a complete response function $\gamma^A(t)$ for absorption. Non-Markovian effects like this can either be neglected completely, which is a good approximation for slowly varying absorption in undoped fiber, or else included in the correlation functions of the reservoirs as given above.

One can best understand the physical meaning of the reservoir operator spectral correlations by considering the effect of these terms on photodetection, which, according to photodetection theory, means a normally ordered field correlation. This involves normally ordered reservoir correlations to lowest order. Inasmuch as these correlations are zero, we conclude that the absorbing reservoirs essentially add no quantum noise that is observable by normal photodetection methods.

B. Waveguide Laser Amplifiers

The equations for gain or laser reservoirs are generally more complex, involving the nonlinear response of atomic impurities added to provide some gain in the fiber medium. A pump process (usually from a semiconductor laser) to maintain the lasing atoms in an inverted state is also involved. In the case of silica fibers, a commonly used lasing transition is provided by erbium impurities.[28] The effect of these gain reservoirs is typically to introduce new types of dispersion, owing to the frequency dependence of the gain.[29] In addition, there are new nonlinear effects that are due to the effects of saturation, which in turn depend on the pumping intensity.

It is possible to develop a detailed theory of erbium laser amplifiers. However, in this paper we shall treat the simplest possible quantum theory of a traveling-wave quantum-limited laser amplifier. More details of the quantum theory, including nonlinear effects, are treated elsewhere.[30] However, the simple theory presented here provides a microscopic justification for observed quantum-noise effects in fiber amplifier chains. In particular, it reproduces the results of the phenomenological theory of Gordon and Haus,[4] which is known to give predictions in accord with soliton transmission experiments. The resultant Gordon–Haus jitter can be reduced through the use of filtering techniques. Assuming that the laser amplifier is polarization insensitive, we again omit the polarization index. The reservoir variable $\hat{\sigma}_\mu = |1\rangle_\mu\langle 2|_\mu$ is an atomic transition operator, which induces a near-resonant atomic transition from an upper to a lower state, with two-level transitions having an assumed density of $\rho(\omega,x)$ in position and resonant angular frequency ω.

We model these quantum effects here by including gain reservoirs in the Hamiltonian, coupled by a frequency-dependent term $G(\omega,x)$ to the radiating field. Here the gain terms $\hat{\sigma}^{\pm}(\omega,x,t)$ represent the raising and lowering Pauli field operators for two-level lasing transitions at frequency ω. In more detail, we have gain given by an interaction Hamiltonian:

$$\hat{H}_G' = \hbar\int_{-\infty}^{\infty}\mathrm{d}x\int_0^\infty \mathrm{d}\omega\left\{[\hat{\Psi}\hat{\sigma}^+(\omega,x)G(\omega,x) + \mathrm{h.c.}] + \frac{\omega-\omega_0}{2}\sigma^z(\omega,x)\right\}, \quad (4.16)$$

where the atomic raising and lowering field operators, $\hat{\sigma}^{\pm}$, are defined in terms of discrete Pauli operators by

$$\hat{\sigma}^+(\omega,x,t) = \frac{1}{\sqrt{\rho(\omega,x)}}\sum_\mu |2\rangle\langle 1|_\mu \exp(-i\omega_0 t) \times \delta(x-x_\mu)\delta(\omega-\omega_\mu),$$

$$\hat{\sigma}^-(\omega,x,t) = \frac{1}{\sqrt{\rho(\omega,x)}}\sum_\mu |1\rangle\langle 2|_\mu \exp(i\omega_0 t) \times \delta(x-x_\mu)\delta(\omega-\omega_\mu),$$

$$\hat{\sigma}^z(\omega,x,t) = \frac{1}{\rho(\omega,x)}\sum_\mu [|2\rangle\langle 2| - |1\rangle\langle 1|]_\mu \times \delta(x-x_\mu)\delta(\omega-\omega_\mu). \quad (4.17)$$

These operators are, in general, time dependent in the Heisenberg picture but have the equal-time commutation relations

$$[\hat{\sigma}^+(t,\omega,x),\hat{\sigma}^-(t,\omega',x')] = \hat{\sigma}^z(t,\omega,x) \times \delta(x-x')\delta(\omega-\omega'). \quad (4.18)$$

In the limit of complete inversion, with linear response and pure inhomogeneous broadening,

$$\frac{\partial}{\partial t}\hat{\sigma}^{-}(t,\omega,x) = -i(\omega-\omega_0)\hat{\sigma}^{-}(t,\omega,x) + i\hat{\sigma}^{z}(t,\omega,x)G(\omega,x)\hat{\Psi}(t,x). \tag{4.19}$$

Hence the solutions in the amplifier case are

$$\hat{\sigma}^{-}(t,\omega,x) = \hat{\sigma}^{-}(t_0,\omega,x)\exp[-i(\omega-\omega_0)(t-t_0)] + iG(\omega,x)\int_{t_0}^{t}\exp[-i(\omega-\omega_0) \times (t-t')]\hat{\sigma}^{z}(t'\omega,x)\hat{\Psi}(t',x)\mathrm{d}t'. \tag{4.20}$$

With complete inversion, $\langle\hat{\sigma}^{z}(t_0,\omega,x)\rangle = 1$, so the initial correlations for the reservoir variables in the far past ($t_0 \to -\infty$) are given by

$$\langle\hat{\sigma}^{+}(t_0,\omega,x)\hat{\sigma}^{-}(t_0,\omega',x')\rangle = \delta(x-x')\delta(\omega-\omega'),$$
$$\langle\hat{\sigma}^{-}(t_0,\omega,x)\hat{\sigma}^{+}(t_0,\omega'x')\rangle = 0. \tag{4.21}$$

We substitute the solution for $\hat{\sigma}^{-}(t,\omega,x)$ into the Heisenberg equation for the field evolution, assuming no depletion of the inversion, and trace over the atomic gain reservoirs. This gives rise to an extra time-dependent term, of the form

$$\begin{aligned}-i\int_0^{\infty}G^{*}(\omega,x)\hat{\sigma}^{-}(t,\omega,x)\mathrm{d}\omega &= \int_0^{\infty}\mathrm{d}\omega|G(\omega,x)|^2\int_{t_0}^{t}\mathrm{d}t'\exp[-i(\omega-\omega_0) \times (t-t')]\hat{\Psi}(t',x) - i\int_0^{\infty}\mathrm{d}\omega G^{*}(\omega,x) \times \exp[-i(\omega-\omega_0)(t-t_0)]\sigma^{-}(t_0,\omega,x) \\ &= \int_0^{\infty}\mathrm{d}t''\gamma^{G}(t'',x)\hat{\Psi}(t-t'',x) + \hat{\Gamma}^{G}(t,x),\end{aligned} \tag{4.22}$$

where $t'' = t - t'$, as before. This gives

$$\gamma^{G}(t,x) \approx \Theta(t)\int_{-\infty}^{+\infty}\mathrm{d}\omega|G(\omega,x)|^2\exp[-i(\omega-\omega_0)t],$$

$$\hat{\Gamma}^{G}(t,x) \approx -i\int_{-\infty}^{\infty}\mathrm{d}\omega G^{*}(\omega,x)\exp[-i(\omega-\omega_0) \times (t-t_0)]\sigma^{-}(t_0,\omega,x). \tag{4.23}$$

Fourier transforming the response function gives

$$\tilde{\gamma}^{G}(\omega,x) = \int\gamma^{G}(t,x)\exp(i\omega t)\mathrm{d}t = \gamma^{G}(\omega,x) + i\gamma^{G\prime\prime}(\omega,x), \tag{4.24}$$

and the (real) resonant amplitude gain coefficient is

$$\gamma^{G}(\omega,x) = \pi|G(\omega+\omega_0,x)|^2. \tag{4.25}$$

As with the loss case, $\hat{\Gamma}^{G}(t,x)$ behaves as a stochastic term because of the random initial conditions. The corresponding correlation functions are

$$\begin{aligned}\langle\hat{\Gamma}^{G\dagger}(t',x')\hat{\Gamma}^{G}(t,x)\rangle &= \int_0^{\infty}\mathrm{d}\omega|G(\omega,x)|^2\exp[i(\omega-\omega_0)(t-t')]\delta(x-x') \\ &= [\gamma^{G}(t-t',x) + \gamma^{G*}(t'-t,x)]\delta(x-x').\end{aligned} \tag{4.26}$$

Fourier transforming these noise sources gives

$$\langle\hat{\Gamma}^{G\dagger}(\omega',x')\hat{\Gamma}^{G}(\omega,x)\rangle = 2\gamma^{G}(\omega,x)\delta(x-x')\delta(\omega-\omega'). \tag{4.27}$$

Taking the uniform fiber in the Wigner–Weiskopff limit as before, so $\gamma^{G} = \gamma^{G}(0,x)$, reduces Eq. (4.27) to

$$\langle\hat{\Gamma}^{G}(t,x)\hat{\Gamma}^{G\dagger}(t',x')\rangle = 0,$$
$$\langle\hat{\Gamma}^{G\dagger}(t,x)\hat{\Gamma}^{G}(t',x')\rangle = 2\gamma^{G}\delta(t-t')\delta(x-x'). \tag{4.28}$$

The dimensions for the amplitude gain γ^{G} are inverse time. On Fourier transforming, the response function can be related to the measured intensity gain $2\,\mathrm{Re}[\tilde{\gamma}^{G}(\omega,x)/v]$ at any frequency offset ω relative to the carrier frequency ω_0. This allows one to obtain the linear gain coefficient for fibers during propagation. As measured laser gain figures can be much greater than the absorption, it is possible to compensate for fiber absorption with relatively short regions of gain. The results presented here are valid only in the linear gain regime. More generally, a functional Taylor expansion up to at least third order in the field would be needed to represent the full nonlinear response of the laser amplifier, together with additional quantum-noise terms.

Finally, it is necessary to consider the result of incomplete inversion of an amplifier. Here, the noninverted atoms give rise to absorption, not gain, and will generate additional quantum-noise and absorption response terms. These terms must be treated as in Subsection 4.A, including non-Markovian effects if the absorption line is narrow band. An important consequence is that the measured gain gives only the difference between the gain and the loss, which does not cause any problems with the deterministic response function but does cause difficulties in determining the amplifier quantum noise levels, which can be uniquely determined only through spontaneous fluorescence measurements. Obviously, the lowest quantum-noise levels occur when all the lasing transitions are completely inverted.

The physical meaning of the reservoir operator spectral correlations for the amplifier is clearly quite different from that of the absorber. If we consider the effect of these terms on photodetection as before, which means a normally ordered field correlation, we should look again at the normally ordered correlations of the reservoirs. Because these correlations are no longer zero, we conclude that the amplifying reservoirs emit fluorescent photons as a result of spontaneous emission over the amplifier bandwidth.

5. COMBINED HEISENBERG EQUATIONS

Coupling linear gain and absorption reservoirs in this way to the Raman-modified Heisenberg equation leads to a generalized quantum nonlinear Schrödinger equation.

Such equations are sometimes called quantum Langevin equations. In the present case of single polarization, the resultant field equations are

$$\left(v\frac{\partial}{\partial x}+\frac{\partial}{\partial t}\right)\hat{\Psi}(t,x) = -\int_0^\infty \mathrm{d}t'\,\gamma(t',x)\hat{\Psi}(t-t',x)+\hat{\Gamma}(t,x) + i\left\{\frac{\omega''}{2}\frac{\partial^2}{\partial x^2}+\int_{0-}^\infty \mathrm{d}t'\chi(t') \times[\hat{\Psi}^\dagger\hat{\Psi}](t-t',x)+\hat{\Gamma}^R(t,x)\right\}\hat{\Psi}(t,x). \quad (5.1)$$

In Eq. (5.1),

$$\gamma(t,x)=\gamma^A(t,x)-\gamma^G(t,x)+i\Delta\omega(x)\delta(t) \quad (5.2)$$

is a net linear response function that is due to coupling to linear gain–absorption reservoirs, including the effects of a spatially varying refractive index. The reponse function can be Fourier transformed, giving $\tilde{\gamma}(\omega,x)=\gamma(\omega,x)+i\gamma''(\omega,x)$, where $\gamma(\omega,x)<0$ for gain and $\gamma(\omega,x)>0$ for absorption. Similarly, $\hat{\Gamma}(t,x)$ is the linear quantum noise that is due to gain and absorption. The actual measured intensity gain at frequency $\omega+\omega_0$ is given in units of inverse meters by

$$\frac{\partial \ln I}{\partial x}=2[\gamma^G(\omega,x)+\gamma^A(\omega,x)]/v. \quad (5.3)$$

The stochastic terms have the correlations

$$\langle\hat{\Gamma}^{R\dagger}(\omega',x')\hat{\Gamma}^R(\omega,x)\rangle = 2\chi''(x,|\omega|)[n_{\mathrm{th}}(|\omega|)+\Theta(-\omega)]\delta(x-x')\times\delta(\omega-\omega'),$$

$$\langle\hat{\Gamma}^\dagger(\omega',x')\hat{\Gamma}(\omega,x)\rangle = 2\gamma^G(\omega,x)\delta(x-x')\delta(\omega-\omega'),$$

$$\langle\hat{\Gamma}(\omega,x)\hat{\Gamma}^\dagger(\omega',x')\rangle = 2\gamma^A(\omega,x)\delta(x-x')\delta(\omega-\omega'), \quad (5.4)$$

where we have introduced minimal linear quantum-noise terms $\hat{\Gamma}$ and $\hat{\Gamma}^\dagger$ for the gain–absorption reservoirs and where thermal photons have been neglected (because usually $\hbar\omega_0 \gg kT$, as we explained in Section 4). Equation (5.1) can easily be generalized to include nonlinear absorption or laser saturation effects relevant to amplifiers with intense fields, but these terms are omitted here for simplicity.

This complete Heisenberg equation gives a consistent quantum theoretical description of dispersion, nonlinear refractive index, Raman/guided wave acoustic Brillouin scattering, linear gain, and absorption. It is important to notice that the reservoir correlations have a simple physical interpretation, especially in the zero-temperature limit. Normally ordered noise correlations occur when there is gain; antinormally ordered correlations, when there is absorption. This is why the normally ordered Raman noise correlations vanish at zero temperature for positive frequencies. At low temperatures, Raman processes cause absorption to occur only at positive detunings from a pump frequency. Thermal correlations have a more classical behavior and occur for both types of operator ordering.

It is often useful to do calculations in a simpler model, in which we include the effects of uniform gain and loss in a moving frame. This modeling can be carried out either with a standard moving frame ($x_v=x-vt$) or with a propagative time ($t_v=t-x/v$) as in the original Gordon–Haus calculations. For propagative calculations it is most convenient to use photon flux operators:

$$\hat{\Phi}(t_v,x)=\sqrt{v}\hat{\Psi}(t,x). \quad (5.5)$$

For long pulses, assuming a uniform gain–loss response in the frequency domain, the propagative transformation gives the following approximate equations:

$$\frac{\partial}{\partial x}\hat{\Phi}(t_v,x) = -\int_0^\infty \mathrm{d}t_v'\frac{\gamma(t_v',x)}{v}\hat{\Phi}(t_v-t_v',x) + \hat{\Gamma}(t)\Big/\sqrt{v}+i\left\{-\frac{k''}{2}\frac{\partial^2}{\partial t_v^{\,2}} + \int_0^\infty \mathrm{d}t'\frac{\chi(t_v')}{v^2} \times[\hat{\Phi}^\dagger\hat{\Phi}](t_v-t_v',x)+\frac{1}{v}\hat{\Gamma}^R\right\}\hat{\Phi}(t_v,x). \quad (5.6)$$

In addition, if the pulses are narrow band compared with the gain and loss bandwidths, and the reservoirs are uniform, then the gain and absorption reservoirs are nearly delta correlated, with

$$\langle\hat{\Gamma}^\dagger(t,x_v)\hat{\Gamma}(t',x_v')\rangle = 2\gamma^G\delta(x_v-x_v')\times\delta(t-t')\times\langle\hat{\Gamma}(t,x_v)\hat{\Gamma}^\dagger(t',x_v')\rangle = 2\gamma^A\delta(x_v-x_v')\delta(t-t'). \quad (5.7)$$

It is essentially this set of approximate equations that corresponds to those used to predict the soliton[31] self-frequency shift[32] and related effects[4] in soliton propagation, except for the omission of the Raman reservoir terms.

6. PHASE-SPACE METHODS

The Heisenberg equations are not readily solvable in their present form. To generate numerical equations for analytic calculations or for simulation, operator representation theory can be used. There is more than one possible method, depending on which phase-space representation is used. The $+P$ representation, for example, produces exact results,[1,8,16] provided that phase-space boundary terms are negligible, whereas a truncated Wigner representation[33,34] gives approximate results that are valid in the limit of large photon number. It is important to note that the Wigner method represents symmetrically ordered rather than normally ordered operator products and so has finite quantum-noise terms even for a vacuum field. These terms can be thought of as corresponding to the shot noise detected in a homodyne or

local-oscillator measurement, whereas the $+P$ representation represents normally ordered operators and therefore corresponds to direct-detection noise.

Either technique can be used for this problem, each with its characteristic advantages and disadvantages. The $+P$ representation, although it is exact, uses an enlarged phase space, which therefore takes longer to simulate numerically. It includes only normally ordered noise and initial conditions, and this is an advantage in some cases, as the resultant noise is zero in the vacuum state. The Wigner technique is simpler, and for large mode occupations its results are accurate enough for many purposes. However, it has the drawback that it includes symmetrically ordered vacuum fluctuations.

First, we expand the field operators in terms of operators for the free-field modes. Applying the appropriate operator correspondences to the master equation for the reduced density operator $\hat{\rho}_\Psi$ in which the reservoir modes have been traced over, namely,

$$\dot{\hat{\rho}}_\Psi = \mathrm{Tr}_R \dot{\hat{\rho}}_\Psi = \mathrm{Tr}_R \frac{1}{i\hbar}[\hat{H}, \hat{\rho}], \tag{6.1}$$

gives a functional equation for the corresponding operator representation.

In the $+P$ case, the equation is defined on a functional phase space of double the classical dimensions, so that a complete expansion in terms of a coherent-state basis $|\Psi\rangle$ is obtained:

$$\hat{\rho}_\Psi(t) = \int\int P(t, \Psi, \bar{\Psi}) \frac{|\Psi\rangle\langle\bar{\Psi}|}{\langle\bar{\Psi}|\Psi\rangle} \mathrm{d}[\Psi]\mathrm{d}[\bar{\Psi}]. \tag{6.2}$$

The resultant Fokker–Planck equation for the positive distribution $P(t, \Psi, \bar{\Psi})$ has only second-order derivative terms. Sometimes the notation $\Psi^+ = \bar{\Psi}^*$ is used to indicate the stochastic field that corresponds to the Hermitian conjugate of Ψ.

The equation for the Wigner function $W(t, \Psi)$ also contains third- and fourth-order derivative terms, which may be neglected at large photon number. The resultant Fokker–Planck equation in either case can be converted into equivalent Ito stochastic equations for the phase-space variables Ψ (and $\bar{\Psi}$). We can calculate physical quantities by forming the average over many stochastic realizations, or paths, in phase space. For example, in the $+P$ representation, $\langle\bar{\Psi}^*\Psi\rangle_{\mathrm{stochastic}} = \langle\hat{\Psi}^\dagger\hat{\Psi}\rangle_{\mathrm{quantum}}$, whereas, in the Wigner representation, $\langle\Psi^*\Psi\rangle_{\mathrm{stochastic}} = 1/2\langle\hat{\Psi}^\dagger\hat{\Psi} + \hat{\Psi}\hat{\Psi}^\dagger\rangle_{\mathrm{quantum}}$.

It should be clear therefore that the $+P$ representation directly generates an intensity that corresponds to the usual normally ordered intensity that is detected in direct photodetection. The Wigner representation, however, generates an intensity result that includes some vacuum fluctuations. In a computer simulation with a finite number M of modes, we must correct the Wigner result by subtracting $M/2$ from any simulated photon number, or $vM/2$ from any calculated photon flux, to obtain the direct photodetection result. For the calculation of a homodyne measurement, the Wigner method will give the most directly suitable result with symmetric ordering. In this case it is the $+P$ representation that will need correction terms added to it. Once these corrections are made, the two methods will give similar results, although the sampling error may not be identical.

A. Modified Nonlinear Schrödinger Equation

Standard custom in fiber-optics applications[31] involves using the propagative reference frame with the normalized variables: $\tau = (t - x/v)/t_0$ and $\zeta = x/x_0$, where t_0 is a typical pulse duration used for scaling purposes and $x_0 = {t_0}^2/|k''| \sim 1\,\mathrm{km}$ for dispersion-shifted fiber. This change of variables is useful only when slowly varying second-order derivatives involving ζ can be neglected, a condition that occurs for $vt_0/x_0 \ll 1$. For typical values of the parameters used in experiments, this inequality is often well satisfied ($vt_0 \sim 10^{-4}\,\mathrm{m}$). To make comparison with this usage simpler, we make the same transformation for the stochastic equations that are equivalent to our complete operator equations and scale the variables used in a dimensionless form.

For definiteness, we now focus on the spatially uniform case. The resultant equation, which includes gain and loss, is a Raman-modified NLS equation with stochastic noise terms:

$$\begin{aligned}\frac{\partial}{\partial\zeta}\phi(\tau, \zeta) = &-\int_{-\infty}^{\infty} \mathrm{d}\tau' g(\tau-\tau')\phi(\tau', \zeta) + \Gamma(\tau, \zeta) \\ &+ \left[\pm \frac{i}{2}\frac{\partial^2\phi}{\partial\tau^2} + i\int_{-\infty}^{\infty} \mathrm{d}\tau' h(\tau - \tau') \right. \\ &\left. \times \phi^*(\tau', \zeta)\phi(\tau', \zeta) + \Gamma^R(\tau, \zeta)\right]\phi(\tau, \zeta),\end{aligned} \tag{6.3}$$

where $\phi = \Psi\sqrt{vt_0/\bar{n}}$ is a dimensionless photon field amplitude. The photon flux is $|\phi|^2\bar{n}/t_0$, and $\bar{n} = |k''|Ac/(n_2\hbar\omega_c{}^2t_0) = v^2t_0/\chi x_0$ is the typical number of photons in a soliton pulse of width t_0, for scaling purposes. The positive sign in front of the second derivative term applies for anomalous dispersion ($k'' < 0$), which occurs for longer wavelengths, and the negative sign applies for normal dispersion ($k'' > 0$). A similar equation is obtained in the $+P$ case, except that ϕ^* and $\Gamma^{R^*}(\tau, \zeta)$ are replaced by non-complex-conjugate fields, denoted ϕ^+ and $\Gamma^{R+}(\tau, \zeta)$, respectively:

$$\begin{aligned}\frac{\partial}{\partial\zeta}\phi^+(\tau, \zeta) = &-\int_{-\infty}^{\infty} \mathrm{d}\tau' g^*(\tau - \tau')\phi^+(\tau', \zeta) + \Gamma^+(\tau, \zeta) \\ &+ \left[\mp \frac{i}{2}\frac{\partial^2\phi^+}{\partial\tau^2} - i\int_{-\infty}^{\infty} \mathrm{d}\tau' h^*(\tau - \tau') \right. \\ &\left. \times \phi(\tau', \zeta)\phi^+(\tau', \zeta) + \Gamma^{+R}(\tau, \zeta)\right]\phi^+(\tau, \zeta).\end{aligned} \tag{6.4}$$

The equations in ϕ and ϕ^+ have the same additive noises and identical mean values, differing only in the independent parts of the multiplicative noise sources, which therefore generate nonclassical quantum statistics.

The causal linear response function $g(\tau)$ is defined as

$$g(\tau) = \frac{\gamma(\tau t_0)x_0}{v}. \tag{6.5}$$

If the Fourier transform of this function is $\tilde{g}(\Omega) = g(\Omega) + ig'(\Omega)$, then we can relate this to dimensionless intensity gain $\alpha^G(\Omega)$ and loss $\alpha^A(\Omega)$, at a relative (dimensionless) detuning of Ω, by

$$2g(\Omega) = \alpha^A(\Omega) - \alpha^G(\Omega). \tag{6.6}$$

The causal nonlinear response function $h(\tau)$ is normalized such that $\int h(\tau)\mathrm{d}\tau = 1$, and it includes both electronic and Raman nonlinearities:

$$h(\tau) = h^E(\tau) + h^R(\tau) = \frac{\bar{n}x_0\chi(\tau t_0)}{v^2}. \tag{6.7}$$

The Raman response function $h^R(\tau)$ causes effects such as the soliton self-frequency shift.[32] The response function Fourier transform is given by

$$\tilde{h}(\Omega) = \int \mathrm{d}t\, \exp(i\Omega\tau)h(\tau) = h'(\Omega) + ih''(\Omega). \tag{6.8}$$

This definition has the property that the value of $\tilde{h}(\Omega) = \tilde{h}(\omega t_0)$ is a dimensionless number, which depends on the frequency ω only, independently of the time scale used for normalization. The Raman gain, whose spectrum has been extensively measured,[22] can be modeled as a sum of n Lorentzians, as explained in Section 3 and as illustrated in Fig. 1.

This expansion as n Lorentzians gives a response function of the form

$$h^R(t/t_0) = \Theta(t)\sum_{j=0}^{n} F_j\delta_j t_0 \exp(-\delta_j t)\sin(\omega_j t). \tag{6.9}$$

It is most convenient to express these Lorentzians in terms of dimensionless parameters $\Omega_j = \omega_j t_0$ and $\Delta_j = \delta_j t_0$, giving

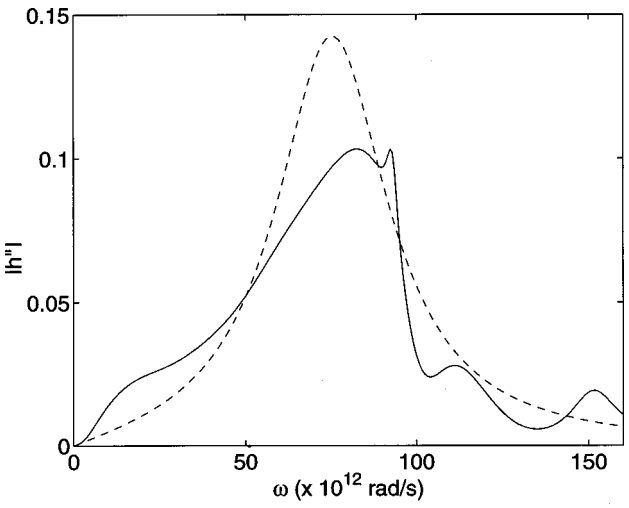

Fig. 1. Parallel polarization Raman gain $|\Im\{\tilde{h}(\omega t_0)\}| = |h''(\omega t_0)|$ for the 11-Lorentzian model (continuous curve) and the single-Lorentzian model (dashed curve) for a temperature of $T = 300$ K.

$$h^R(\tau) = \Theta(\tau)\sum_{j=0}^{n} F_j\Delta_j \exp(-\Delta_j\tau)\sin(\Omega_j\tau). \tag{6.10}$$

Here Δ_j are the equivalent dimensionless widths (corresponding to damping) and Ω_j are the dimensionless center frequencies, all in normalized units. It is useful to compare these results with the dimensionless Raman gain $\alpha^R(\Omega)$ normalized following Gordon,[32] which uses a characteristic time scale of t_0. The relationship of macroscopic coupling $R(\omega)$ to measured Raman gain $\alpha^R(\Omega)$ is $R^2(\omega) = \chi\alpha^R(\omega t_0)/2\pi$. It follows that the dimensionless gain function is

$$\alpha^R(\Omega) = 2|h''(\Omega)|. \tag{6.11}$$

These stochastic partial differential equations can be discretized and, without any further approximation, can be numerically simulated[33,35] with a split-step Fourier integration routine. The equations include all the currently known noise physics that is significant in soliton propagation, including effects such as the soliton self-frequency shift. Guided acoustic wave Brillouin scattering[23–25] noise sources are included in the Raman gain function. They have little effect on the position of an isolated soliton but are important for long-range soliton collision effects[26] that occur in pulse trains.

B. Initial Conditions

The initial conditions for the calculations could involve any required quantum state if the $+P$ representation is used. In the case of the Wigner equations, only a subset of possible states can be represented with a positive probability distribution. The usual initial condition is the multimode coherent state, as this is the simplest model for the output of mode-locked lasers. In general, there could be extra technical noise. We note that the choice of a coherent state is the simplest known model of a laser sources; to represent it in the $+P$ distribution is simple; one just takes

$$\phi_P(\tau, 0) = [\,\phi_P{}^+(\tau, 0)]^* = \langle\hat{\phi}(\tau, 0)\rangle. \tag{6.12}$$

In the Wigner case, which corresponds to symmetric operator ordering, one must also include complex quantum vacuum fluctuations to represent operator fields correctly. For coherent inputs, the Wigner vacuum fluctuations are Gaussian and are correlated as

$$\langle\,\phi_W(\tau, 0)\rangle = \langle\hat{\phi}(\tau, 0)\rangle,$$

$$\langle\Delta\phi_W(\tau, 0)\Delta\phi_W{}^*(\tau', 0)\rangle = \frac{1}{2\bar{n}}\delta(\tau - \tau'). \tag{6.13}$$

We note that these equations imply that an appropriate correction is made for losses at the input interface, so the mean-field evolution is known at the fiber input face.

C. Wigner Noise

Both fiber loss and the presence of a gain medium contribute quantum noise to the equations in this symmetrically ordered representation. The complex gain–absorption noise enters the Wigner equation through an additive stochastic term Γ, whose correlations one obtains by averaging the normally and antinormally ordered reservoir cor-

relation functions already determined, together with appropriate variable changes. This symmetrically ordered noise source is present for both gain and loss reservoirs. Thus,

$$\langle \Gamma(\Omega,\zeta)\Gamma^*(\Omega',\zeta')\rangle = \frac{[\alpha^G(\Omega)+\alpha^A(\Omega)]}{2\bar{n}} \times \delta(\zeta-\zeta')\delta(\Omega-\Omega'), \quad (6.14)$$

where $\Gamma(\Omega,\zeta)$ is the Fourier transform of the noise source:

$$\Gamma(\Omega,\zeta) = \frac{1}{\sqrt{2\pi}}\int_{-\infty}^{\infty} d\tau\Gamma(\tau,\zeta)\exp(i\Omega\tau),$$

$$\Gamma^*(\Omega,\zeta) = \frac{1}{\sqrt{2\pi}}\int_{-\infty}^{\infty} d\tau\Gamma^*(\tau,\zeta)\exp(-i\Omega\tau). \quad (6.15)$$

Similarly, the real Raman noise, which appears as a multiplicative stochastic variable Γ^R, has correlations

$$\langle \Gamma^R(\Omega,\zeta)\Gamma^{R^*}\rangle(\Omega',\zeta')\rangle = \frac{\alpha^R(|\Omega|)}{\bar{n}}[n_{\rm th}(|\Omega|/t_0)+(1/2)] \times \delta(\zeta-\zeta')\delta(\Omega-\Omega'). \quad (6.16)$$

Thus the Raman noise is strongly temperature dependent, but it also contains a spontaneous component that provides vacuum fluctuations even at $T=0$. As the spontaneous component can occur through coupling to either a gain or a loss reservoir, in a symmetrically ordered representation it is present for both positive and negative frequency detunings.

It must be remembered here that the noise terms in the Wigner representation do not correspond to normally ordered correlations and so have no direct interpretation in terms of photodetection experiments. Any predictions made with this method of calculation need to be corrected by subtraction of the appropriate commutators to convert the results into a normally ordered form. This is the reason why there is no obvious distinction between the amplifier and absorber cases.

D. $+P$ Noise

The $+P$ representation is a useful alternative strategy for deriving complex-number equations, because it does not require truncation of higher-order derivatives in a Fokker–Planck equation and corresponds directly to observable normally ordered, time-ordered operator correlations. It has no vacuum fluctuation terms. Provided that the phase-space boundary terms are negligible, one can obtain a set of c-number stochastic differential equations in a phase space of double the usual classical dimensions. These are similar to the classical equations. Here the additive stochastic term is as before, except that it depends only on gain term α^G; the conjugate term Γ^* is used in the ϕ^+ equation:

$$\langle \Gamma(\Omega,\zeta)\Gamma^*(\Omega',\zeta')\rangle = \frac{\alpha^G(\Omega)}{\bar{n}}\delta(\zeta-\zeta')\delta(\Omega-\Omega'). \quad (6.17)$$

Because this representation is normally ordered, the only noise sources present are due to the gain reservoirs. There is no vacuum noise term for the absorbing reservoirs, because absorption simply maps a coherent state into another coherent state.

The complex terms Γ^R and Γ^{R+} include both Raman and electronic terms [through $h'(\Omega)$]. As elsewhere in this paper, we regard $\Gamma^{R+}(\Omega,\zeta)$ as a Hermitian conjugate Fourier transform (with the opposite sign frequency exponent):

$$\Gamma^+(\Omega,\zeta) = \frac{1}{\sqrt{2\pi}}\int_{-\infty}^{\infty} d\tau\Gamma^+(\tau,\zeta)\exp(-i\Omega\tau). \quad (6.18)$$

This quantity is not the same as $\Gamma^{R*}(\Omega,\zeta)$, as it involves a noise source that is in general independent. In some cases in which classical noise is dominant (and nonclassical squeezing is negligible), we can ignore this fact and approximately set $\Gamma^{R+}(\Omega,\zeta)=\Gamma^{R*}(\Omega,\zeta)$. More generally, we obtain the following results:

$$\begin{aligned}\langle \Gamma^R(\Omega,\zeta)\Gamma^R(\Omega',\zeta')\rangle &= \delta(\zeta-\zeta')\delta(\Omega+\Omega') \times\{[n_{\rm th}(|\Omega|/t_0)+1/2] \times \alpha^R(|\Omega|)-ih'(\Omega)\}/\bar{n},\\ \langle \Gamma^{R+}(\Omega',\zeta')\Gamma^R(\Omega,\zeta)\rangle &= \delta(\zeta-\zeta')\delta(\Omega-\Omega') \times[n_{\rm th}(|\Omega|/t_0) + \Theta(-\Omega)]\alpha^R(|\Omega|)/\bar{n}.\end{aligned} \quad (6.19)$$

Equations (6.19) are the expected result, as they state that when $\Omega<0$ the spectral intensity of noise that is due to the Stokes process, in which a photon is downshifted in frequency by an amount Ω with the production of a phonon of the same frequency, is proportional to $n_{\rm th}+1$. However, the anti-Stokes process in which a phonon is absorbed ($\Omega>0$) is proportional only to $n_{\rm th}$. Thus at low temperatures the only direct noise effect is that which is due to the Stokes process, which can be interpreted physically as originating in spontaneous photon emission that is detectable through photodetection.

As one might expect, the two forms of equation are identical at high phonon occupation numbers when classical noise is so large that it obscures the differences that are due to the operator orderings of the two representations. Another, less obvious, result is that the two equations have identical additive noise sources, provided that gain and loss are balanced. To understand this, we can see that, in the absence of any net gain or loss, the difference in the operator correlations that is due to ordering is a constant, which is contained in the initial conditions.

However, when gain and loss are not equal, the additive noise sources are quite different. In particular, the Wigner representation has noise contributions from both types of reservoir. However, the normally ordered $+P$ method leads to additive noise only when there is a real fluorescent field present, which is detectable through photodetection. This field corresponds physically to some kind of gain, either because of the presence of an amplifier or through Raman effects.

In general, the Wigner and $+P$ reservoir correlations are obtainable simply by examination of the expectation values of the Heisenberg reservoir terms, with symmetric and normal ordering, respectively. The additional term proportional to $h'(\Omega)$ in the $+P$ noise terms is due to dispersive nonlinear effects and gives rise to a nonclassical noise source that is responsible for the observed quantum-squeezing effects. Extensions required to treat polarization-dependent Raman scattering are given elsewhere.[14]

7. CONCLUSIONS

Our major conclusion is that quantum-noise effects that are due to the intrinsic finite-temperature phonon reservoirs and finite-bandwidth amplification or absorption can be readily modeled with stochastic equations. The equations themselves have the usual classical form, together with correction terms that we can describe as quantum-noise terms. The precise form of the correction terms depends in detail on the representation employed (although this difference is purely due to operator ordering) as well as on the physical origin of the reservoir couplings. These correction terms can be non-Markovian or nonuniform in space. The generation of the corresponding stochastic noises is a straightforward numerical procedure and generally is much simpler than the use of noncommuting operators. By contrast, the original operator equations have no practical numerical solution in most cases because of the exponential growth of the dimension of the underlying Hilbert space with the number of modes and photons involved.

Detailed applications to short-pulse soliton communications will be given in a subsequent paper.[6] In general, the increasing bandwidth, reduced pulse energies, and greater demands placed on fiber communications and sensors mean that these quantum limits are becoming increasingly important. Already, limits set by quantum amplifiers are known to have great significance in long-distance laser-amplified communications systems. We note that the quantum theory given here also establishes the levels of quantum noise in silica fibers in more-general situations, for example, for dispersion-managed fiber communications[36,37] and for fiber ring lasers with relatively low gain.[38] Similarly, these equations set the limits for experiments that use spectral filtering and related techniques to generate sub-shot-noise pulses[39,40] in optical fibers.

ACKNOWLEDGMENT

We acknowledge helpful comments on this paper by Wai S. Man. J. F. Corney acknowledges support from the Danish Technical Research Council (grant 5600-00-0355).

J. F. Corney's e-mail address is jfc@imm.dtu.dk.

REFERENCES

1. S. J. Carter, P. D. Drummond, M. D. Reid, and R. M. Shelby, "Squeezing of quantum solitons," Phys. Rev. Lett. **58**, 1841–1844 (1987).
2. P. D. Drummond and S. J. Carter, "Quantum-field theory of squeezing in solitons," J. Opt. Soc. Am. B **4**, 1565–1573 (1987).
3. M. Rosenbluh and R. M. Shelby, "Squeezed optical solitons," Phys. Rev. Lett. **66**, 153–156 (1991); P. D. Drummond, R. M. Shelby, S. R. Friberg, and Y. Yamamoto, "Quantum solitons in optical fibres," Nature **365**, 307–313 (1993).
4. J. P. Gordon and H. A. Haus, "Random walk of coherently amplified solitons in optical fiber transmission," Opt. Lett. **11**, 665–667 (1986).
5. H. A. Haus and W. S. Wong, "Solitons in optical communications," Rev. Mod. Phys. **68**, 423–444 (1996).
6. J. F. Corney and P. D. Drummond, "Quantum noise in optical fibers. II. Raman jitter in soliton communications," J. Opt. Soc. Am. B **18**, 153–161 (2001).
7. P. D. Drummond, "Electromagnetic quantization in dispersive inhomogeneous nonlinear dielectrics," Phys. Rev. A **42**, 6845–6857 (1990).
8. P. D. Drummond and S. J. Carter, "Quantum-field theory of squeezing in solitons," J. Opt. Soc. Am. B **4**, 1565–1573 (1987); P. D. Drummond, S. J. Carter, and R. M. Shelby, "Time dependence of quantum fluctuations in solitons," Opt. Lett. **14**, 373–375 (1989).
9. B. Yurke and M. J. Potasek, "Solution to the initial value problem for the quantum nonlinear Schrödinger equation," J. Opt. Soc. Am. B **6**, 1227–1238 (1989).
10. P. D. Drummond and M. Hillery, "Quantum theory of dispersive electromagnetic modes," Phys. Rev. A **59**, 691–707 (1999).
11. E. Power and S. Zienau, "Coulomb gauge in nonrelativistic quantum electrodynamics and the shape of spectral lines," Philos. Trans. R. Soc. London, Ser. A **251**, 427–454 (1959); R. Loudon, *The Quantum Theory of Light* (Clarendon, Oxford, 1983).
12. M. Hillery and L. D. Mlodinow, "Quantization of electrodynamics in nonlinear dielectric media," Phys. Rev. A **30**, 1860–1865 (1984).
13. N. Bloembergen, *Nonlinear Optics* (Benjamin, New York, 1965).
14. P. D. Drummond, "Quantum theory of fiber-optics and solitons," in *Coherence and Quantum Optics VII*, J. Eberly, L. Mandel, and E. Wolf, eds. (Plenum, New York, 1996), pp. 323–332.
15. G. P. Agrawal, *Nonlinear Fiber Optics*, 2nd ed. (Academic, San Diego, Calif., 1995), pp. 28–59.
16. S. J. Carter and P. D. Drummond, "Squeezed quantum solitons and Raman noise," Phys. Rev. Lett. **67**, 3757–3760 (1991).
17. F. X. Kartner, D. J. Dougherty, H. A. Haus, and E. P. Ippen, "Raman noise and soliton squeezing," J. Opt. Soc. Am. B **11**, 1267–1276 (1994).
18. Y. Lai and S.-S. Yu, "General quantum theory of nonlinear optical-pulse propagation," Phys. Rev. A **51**, 817–829 (1995); S.-S. Yu and Y. Lai, "Impacts of self-Raman effect and third-order dispersion on pulse squeezed state generation using optical fibers," J. Opt. Soc. Am. B **12**, 2340–2346 (1995).
19. T. von Foerster and R. J. Glauber, "Quantum theory of light propagation in amplifying media," Phys. Rev. A **3**, 1484–1511 (1971); I. A. Walmsley and M. G. Raymer, "Observation of macroscopic quantum fluctuations in stimulated Raman scattering," Phys. Rev. Lett. **50**, 962–965 (1983).
20. M. D. Levenson, *Introduction to Nonlinear Laser Spectroscopy* (Academic, New York, 1982).
21. P. Dean, "The vibrational properties of disordered systems: numerical studies," Rev. Mod. Phys. **44**, 127–168 (1972).
22. R. H. Stolen, C. Lee, and R. K. Jain, "Development of the stimulated Raman spectrum in single-mode silica fibers," J. Opt. Soc. Am. B **1**, 652–657 (1984); D. J. Dougherty, F. X. Kartner, H. A. Haus, and E. P. Ippen, "Measurement of the Raman gain spectrum of optical fibers," Opt. Lett. **20**, 31–33 (1995); R. H. Stolen, J. P. Gordon, W. J. Tomlinson, and H. A. Haus, "Raman response function of silica-core fibers," J. Opt. Soc. Am. B **6**, 1159–1166 (1989).
23. R. M. Shelby, M. D. Levenson, and P. W. Bayer, "Guided

acoustic-wave Brillouin scattering," Phys. Rev. B **31**, 5244–5252 (1985).
24. R. M. Shelby, P. D. Drummond, and S. J. Carter, "Phase-noise scaling in quantum soliton propagation," Phys. Rev. A **42**, 2966–2796 (1990).
25. K. Bergman, H. A. Haus, and M. Shirasaki, "Analysis and measurement of GAWBS spectrum in a nonlinear fiber ring," Appl. Phys. B **55**, 242–249 (1992).
26. K. Smith and L. F. Mollenauer, "Experimental observation of soliton interaction over long fiber paths: discovery of a long-range interaction," Opt. Lett. **14**, 1284–1286 (1989); E. M. Dianov, A. V. Luchnikov, A. N. Pilipetskii, and A. M. Prokhorov, "Long-range interaction of picosecond solitons through excitation of acoustic waves in optical fibers," Appl. Phys. B **54**, 175–180 (1992).
27. S. H. Perlmutter, M. D. Levenson, R. M. Shelby, and M. B. Weissman, "Inverse-power-law light scattering in fused-silica optical fiber," Phys. Rev. Lett. **61**, 1388–1391 (1988); "Polarization of quasielastic light scattering in fused-silica optical fiber," Phys. Rev. B **42**, 5294–5305 (1990).
28. R. J. Mears, L. Reekie, I. M. Jauncey, and D. N. Payne, "Low-noise erbium-doped fibre amplifier operating at 1.54 μm," Electron. Lett. **23**, 1026–1028 (1987).
29. E. Desurvire, *Erbium-Doped Fiber Amplifiers, Principles and Applications* (Wiley, New York, 1993).
30. P. D. Drummond and M. G. Raymer, "Quantum theory of propagation of nonclassical radiation in a near-resonant medium," Phys. Rev. A **44**, 2072–2085 (1991).
31. L. F. Mollenauer, "Solitons in optical fibers and the soliton laser," Philos. Trans. R. Soc. London A **15**, 437–450 (1985); L. F. Mollenauer, R. H. Stolen, and J. P. Gordon, "Experimental observation of picosecond pulse narrowing and solitons in optical fibers," Phys. Rev. Lett. **45**, 1095–1098 (1980).
32. J. P. Gordon, "Theory of the soliton self-frequency shift," Opt. Lett. **11**, 662–664 (1986); F. M. Mitschjke and L. F. Mollenauer, "Discovery of the soliton self-frequency shift," Opt. Lett. **11**, 659–661 (1986).
33. P. D. Drummond and A. D. Hardman, "Simulation of quantum effects in Raman-active waveguides," Europhys. Lett. **21**, 279–284 (1993); P. D. Drummond and W. Man, "Quantum noise in reversible soliton logic," Opt. Commun. **105**, 99–103 (1994).
34. S. J. Carter, "Quantum theory of nonlinear fiber optics: phase-space representations," Phys. Rev. A **51**, 3274–3301 (1995).
35. M. J. Werner and P. D. Drummond, "Robust algorithms for solving stochastic partial differential equations," J. Comput. Phys. **132**, 312–326 (1997).
36. N. J. Smith, N. J. Doran, W. Forysiak, and F. M. Knox, "Soliton transmission using periodic dispersion compensation," J. Lightwave Technol. **15**, 1808–1822 (1997).
37. T. I. Lakoba and D. J. Kaup, "Influence of the Raman effect on dispersion-managed solitons and their interchannel collisions," Opt. Lett. **24**, 808–810 (1999).
38. S. Namiki, C. X. Yu, and H. A. Haus, "Observation of nearly quantum-limited timing jitter in an all-fiber ring laser," J. Opt. Soc. Am. B **13**, 2817–2823 (1996); B. C. Collings, K. Bergman, and W. H. Knox, "Stable multigigahertz pulse-train formation in a short-cavity passively harmonic mode-locked erbium/ytterbium fiber laser," Opt. Lett. **23**, 123–125 (1998).
39. S. R. Friberg, S. Machida, M. J. Werner, A. Levanon, and T. Mukai, "Observation of optical soliton photon-number squeezing," Phys. Rev. Lett. **77**, 3775–3778 (1996); S. Spalter, M. Burk, U. Strossner, M. Bohm, A. Sizmann, and G. Leuchs, "Photon number squeezing of spectrally filtered sub-picosecond optical solitons," Europhys. Lett. **38**, 335–340 (1997); D. Krylov and K. Bergman, "Amplitude-squeezed solitons from an asymmetric fiber interferometer," Opt. Lett. **23**, 1390–1392 (1998).
40. M. J. Werner, "Raman-induced photon correlations in optical fiber solitons," Phys. Rev. A **60**, R781–R784 (1999).